

Research Article

Lane Changing Trajectory Planning and Tracking Controller Design for Intelligent Vehicle Running on Curved Road

Lie Guo,¹ Ping-Shu Ge,² Ming Yue,¹ and Yi-Bing Zhao¹

¹ School of Automotive Engineering, State Key Laboratory of Structural Analysis for Industrial Equipment, Dalian University of Technology, Dalian 116024, China

² College of Electromechanical & Information Engineering, Dalian Nationalities University, Dalian 116600, China

Correspondence should be addressed to Ping-Shu Ge; gps@dlnu.edu.cn

Received 29 October 2013; Accepted 18 December 2013; Published 9 January 2014;

Academic Editor: Rui Mu

Copyright © 2014 Lie Guo et al. This is an open access article distributed under the Creative Commons Attribution License, which permits unrestricted use, distribution, and reproduction in any medium, provided the original work is properly cited.

To enhance the active safety and realize the autonomy of intelligent vehicle on highway curved road, a lane changing trajectory is planned and tracked for lane changing maneuver on curved road. The kinematics model of the intelligent vehicle with nonholonomic constraint feature and the tracking error model are established firstly. The longitudinal and lateral coupling and the difference of curvature radius between the outside and inside lane are taken into account, which is helpful to enhance the authenticity of desired lane changing trajectory on curved road. Then the trajectory tracking controller of closed-loop control structure is derived using integral backstepping method to construct a new virtual variable. The Lyapunov theory is applied to analyze the stability of the proposed tracking controller. Simulation results demonstrate that this controller can guarantee the convergences of both the relative position tracking errors and the position tracking synchronization.

1. Introduction

Intelligent vehicle has become a hot topic worldwide in recent years. So far, several national and international research programs have been initiated, such as advanced safety vehicle (ASV), intelligent vehicle highway system (IVHS), or the partners for advanced transit and highways (PATH) program, whose main goals are to increase the safety and efficiency in normal traffic environments [1]. An intelligent vehicle should possess the following three abilities simultaneously. The first ability is to recognize the driving environments like the driver does using different types of sensors, such as lane detection and obstacle detection [2]. The second is to realize its longitudinal control so as to keep in the longitudinal direction [3]. The third ability is to steer so as to guide the vehicle along reference trajectories at all possible speeds even in the presence of disturbances [4, 5]. Therein, the lane changing maneuver is one of the extensive investigated automatic driving operations for intelligent vehicles once the optimized trajectory is planned [6]. This

paper focuses on the safety of lane changing for intelligent vehicle on curved roads by tracking the planned trajectory.

The lane changing maneuver is carried out by planning the reference trajectory according to the vehicle states and road information, and then the control laws are designed using onboard sensors to track this virtual trajectory [7]. The trapezoidal acceleration profile resultant trajectory has been known as generating the least possible lateral acceleration on the vehicle [8]. To meet the restriction of the various curvature and change rate for lane changing on curved road, this paper utilizes the trajectory planning method based on trapezoidal acceleration profile. Once the virtual trajectory is planned, the lane changing controller is designed to track this trajectory [9]. For example, Hatipoglu et al. [10] reported the design of an automated lane changing controller with a two-layer hierarchical architecture. Ammoun et al. [11] drew an area of the virtual desire lane changing trajectory by adding speed or acceleration constraints. Lee et al. [12] proposed an integrated lane change driver model and used

closed-loop simulation of the ESC system to control lane changing and lane following maneuvers.

However, the lane changing controllers introduced above depend on the fact that lane changing maneuvers mainly take place on straight road segment. While on curved road, the situation is different with straight road. Toledo-Moreo and Zamora-Izquierdo [13] proposed an interactive multiple model-based method for predicting lane changes in highways. Inspired by the observation that any change in the road curvature affects the vehicle lateral dynamics, Ho et al. [14] realized the lane keeping and lane changing control by using the same controller. Their algorithm incorporates the curvature of a virtual road, the actual steering angle, and the vehicle lateral model to estimate the vehicle position. Ren et al. [7] planned the lane changing trajectory of vehicle on a circular curved road considering the curvature difference between inside and outside lanes. Then the reference yaw angle, yaw rate, and yaw angle acceleration were derived, and the yaw-rate-tracking controller was designed to realize the lane changing maneuvers by applying nonsingular terminal sliding mode technology.

Most of those lane changing maneuvers researched above ignore the influence of lane curvature change and the vehicle longitudinal velocity on lane changing trajectory. This paper aims at the study of the automated lane changing on curved road, where the curvatures of the outside and inside lane are not zero, nor equal. The main contributions of this paper are as follows: (1) a trajectory planning method suitable for curved road is proposed based on trapezoidal acceleration profile; (2) the coupled function of the vehicle's longitudinal and lateral motion on lane changing trajectory is taken into account, namely, the curvature radius of which is a vector in lane changing maneuver; (3) on this basis, the trajectory tracking control algorithm is designed using integral backstepping with Lyapunov theory.

The remainder of this paper is organized as follows. The lane change trajectory is planned in Section 2. Section 3 builds the vehicle kinematics and tracking error model and then designs the trajectory tracking controller. Simulation and discussion are given in Section 4. Section 5 concludes this paper.

2. Trajectory Planning for Lane Changing

Lane change reference trajectories play a crucial role in the lane change maneuver. Currently, the commonly used trajectories for lane changing are isokinetic migration lane changing trajectory, arc lane changing trajectory, trapezoidal acceleration lane changing trajectory, sine function lane changing trajectory, and so forth [15]. The trapezoidal acceleration profile resultant trajectory has been known as generating the least possible lateral acceleration on the vehicle. The time requirement for changing lane and the vehicle dynamics can be combined to choose the desired lateral acceleration [7, 16]. This paper utilizes the trajectory planning method based on trapezoidal acceleration profile to meet the restriction of the various curvatures and change

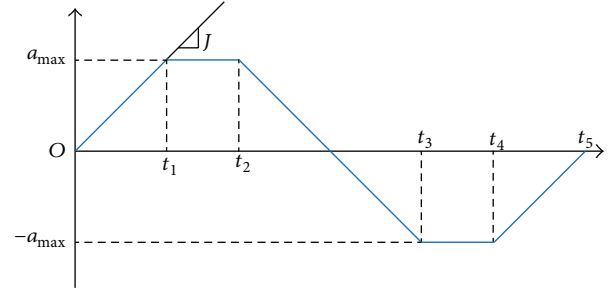


FIGURE 1: Schematic diagram of trapezoidal acceleration profile.

rate for lane changing on curved road. This method regards that the acceleration profile consists of two opposite ladders with the same size, as Figure 1. The lateral acceleration rate is defined as

$$\begin{aligned} \ddot{y}_d(t) = & J_{\max}(t-t_0) \cdot u(t-t_0) - J_{\max}(t-t_1) \cdot u(t-t_1) \\ & - J_{\max}(t-t_2) \cdot u(t-t_2) + J_{\max}(t-t_3) \cdot u(t-t_3) \\ & + J_{\max}(t-t_4) \cdot u(t-t_4) - J_{\max}(t-t_5) \cdot u(t-t_5), \end{aligned} \quad (1)$$

where $\ddot{y}_d(t)$ is the desired vehicle lateral acceleration and J_{\max} denotes the maximum of lateral acceleration rate. $u(t)$ is a unit step function and t is the elapse time of the lane changing maneuver. t_0 denotes the starting time for this maneuver and t_5 denotes the finishing time.

The key times for the lane changing maneuver satisfy the following constraints:

$$\begin{aligned} t_1 &= \frac{a_{\max}}{J_{\max}}, \\ t_2 &= -\frac{a_{\max}}{2J_{\max}} + \frac{\sqrt{(a_{\max}/J_{\max})^2 + 4d_w/a_{\max}}}{2}, \\ t_3 &= 2t_1 + t_2, \\ t_4 &= t_1 + 2t_2, \quad t_5 = 2t_1 + 2t_2, \end{aligned} \quad (2)$$

where d_w is defined as the distance between the outside and inside lane. It is obvious that each time is the function of lateral acceleration and lateral acceleration rate. Once the vehicle lateral acceleration and lateral acceleration rate are determined, the trajectory for lane changing can be planned.

The lane changing trajectory on curved road is planned based on research results for lane changing on straight road segment, assuming that the outside and the inside lane have the same instantaneous center O_R , and the curvature radius R of the outside lane is a constant.

The vehicle's motion state during lane changing on curved road is shown in Figure 2. The inertial coordinate system is established, where O denotes the starting position of vehicle during lane changing. The x -axis is along the tangent of outside lane centerline, while y -axis is in the direction of

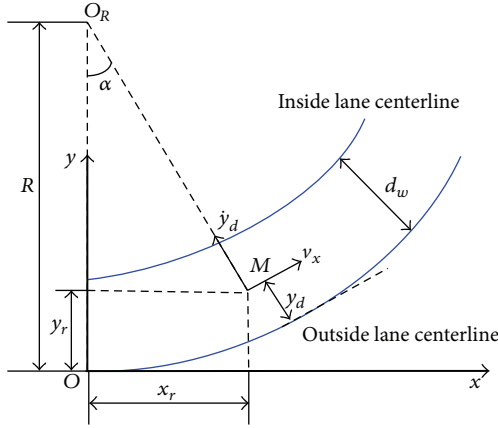


FIGURE 2: Schematic diagram of lane changing trajectory.

instantaneous center O_R . v_x represents the vehicle longitudinal velocity.

The desired lateral velocity and lateral displacement are represented by $\dot{y}_d(t)$ and $y_d(t)$, respectively, and the desired longitudinal velocity of vehicle is denoted by $v_d(t)$. Among that, the longitudinal acceleration $\dot{v}_d(t)$ during lane changing maneuver is shown as follows:

$$\dot{v}_d(t) = \begin{cases} 0 & 0 < t \leq t_1 \\ 0.4(t - t_1) & t_1 < t \leq t_2 \\ 0.2 & t_2 < t \leq t_3 \\ -0.4(t - t_4) & t_3 < t \leq t_4 \\ 0 & t_4 < t \leq t_5 \end{cases} \quad (3)$$

Assuming that the starting time t_0 is zero, then at time t during lane changing procedure, the displacement from the starting lane to the target lane is denoted by $y_d(t)$, so the instantaneous radius of the vehicle's center M yields $R - y_d(t)$, and the angular velocity of M around the instantaneous center O_R is obtained as $v_d(t)/[R - y_d(t)]$. Hence, at time t , the rotated angle of the vehicle around O_R can be calculated by the integral operation as

$$\alpha = \int_0^t \frac{v_d(t)}{R - y_d(t)} dt. \quad (4)$$

Here the values of vehicle's desired motion states at the time t during lane changing maneuver can be derived. Along the x -axis, the desired displacement, velocity, and acceleration can be calculated as

$$\begin{aligned} x_r(t) &= [R - y_d(t)] \sin \alpha, \\ \dot{x}_r(t) &= v_d(t) \cos \alpha - \dot{y}_d(t) \sin \alpha, \\ \ddot{x}_r(t) &= \left[\dot{v}_d(t) - \frac{v_d(t) \dot{y}_d(t)}{R - y_d(t)} \right] \cos \alpha \\ &\quad + \left[\ddot{y}_d(t) + \frac{v_d^2(t)}{R - y_d(t)} \right] \sin \alpha. \end{aligned} \quad (5)$$

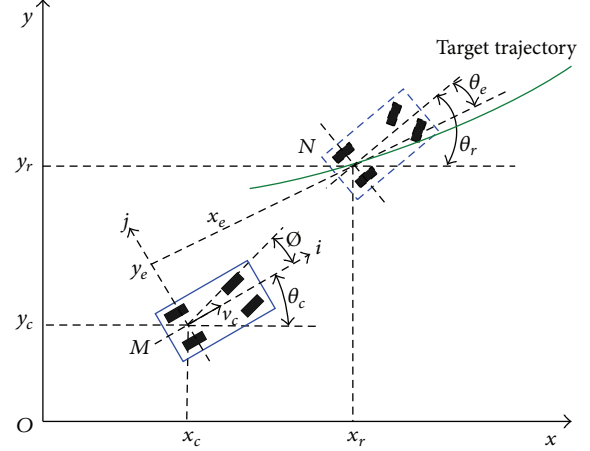


FIGURE 3: Vehicle real posture and the reference posture in world coordinate system.

Along the y -axis, the desired displacement, velocity, and acceleration can be calculated as

$$\begin{aligned} y_r(t) &= R - [R - y_d(t)] \cos \alpha, \\ \dot{y}_r(t) &= v_d(t) \sin \alpha + \dot{y}_d(t) \cos \alpha, \\ \ddot{y}_r(t) &= \left[\dot{v}_d(t) - \frac{v_d(t) \dot{y}_d(t)}{R - y_d(t)} \right] \sin \alpha \\ &\quad + \left[\ddot{y}_d(t) + \frac{v_d^2(t)}{R - y_d(t)} \right] \cos \alpha \end{aligned} \quad (6)$$

and the reference yaw angle and yaw angular velocity can be determined as

$$\begin{aligned} \theta_r(t) &= \arctan \frac{\dot{y}_r(t)}{\dot{x}_r(t)}, \\ \dot{\theta}_r(t) &= \frac{\ddot{y}_r(t) \dot{x}_r(t) - \dot{y}_r(t) \ddot{x}_r(t)}{\dot{x}_r^2(t) + \dot{y}_r^2(t)}. \end{aligned} \quad (7)$$

3. Trajectory Tracking Controller Design

3.1. Vehicle Kinematics and Tracking Error Model. Due to the directionality of the vehicle motion, the vehicle's position and orientation are described by two independent coordinates, which are world coordinate system Oxy and local coordinate system Mij . This paper takes the center of the vehicle driving wheels as the origin of Mij . The position and orientation, namely, the posture of an intelligent vehicle, are shown in Figure 3.

The kinematics model of the vehicle is the starting point to model the kinematics of the lateral and orientation errors. The vehicle model is approximated by the popular Ackerman model [17], regarding the vehicle as rigid body and assuming that the two front wheels turn slightly differentially. Thus, the instantaneous rotation center can be purely computed by

kinematic means. The nonlinear vehicle kinematics model can be described as [18]

$$\dot{p}_c = \begin{bmatrix} \dot{x}_c \\ \dot{y}_c \\ \dot{\theta}_c \end{bmatrix} = \begin{bmatrix} \cos \theta_c & 0 \\ \sin \theta_c & 0 \\ 0 & 1 \end{bmatrix} \begin{bmatrix} v_c \\ \omega_c \end{bmatrix} = J u_c, \quad (8)$$

where $p_c = [x_c \ y_c \ \theta_c]^T \in R^3$ is the vehicle's current posture. $M(x_c \ y_c)$ is the vehicle's current position in Oxy . θ_c is the vehicle's current moving orientation along x -axis anticlockwise; namely, it is the angle between the coordinate system of Oxy and Mij . Assuming that the control vector $u_c = [v_c \ \omega_c]^T \in R^2$, $v_c > 0$, u_c is a function of time t . Here, $v_c \in R$ denotes the linear velocity of the midpoint of the vehicle rear axle, denoted as control point. $\omega_c \in R$ indicates the angular velocity of the intelligent vehicle. Both of them are input variables in the kinematics model. J denotes the velocity Jacobian matrix of the vehicle.

As shown in Figure 1, assuming that $p_r = [x_r \ y_r \ \theta_r]^T \in R^3$ is the vehicle's reference posture, $N(x_r \ y_r)$ indicates the vehicle's reference position, and θ_r denotes its reference moving orientation. It is necessary to define a suitable representation for the vehicle trajectory tracking error. This step is all the more important that an adequate choice significantly facilitates the control design [19]. In order to track a given trajectory smoothly, a path must be computed from a given initial location and heading to some target point on the desired trajectory. A tracking error function is generally defined by a vector between the predictive reference vector and a controlled vehicle traveling vector. The error functions are a velocity equation that is calculated by current posture, which is derived from the velocity equation [20]. Therefore, the relationship between control vector and the posture error should be explained. To achieve the tracking performance of $p_c \rightarrow p_r$ when $t \rightarrow \infty$, the tracking error vector $p_e = [x_e \ y_e \ \theta_e]^T \in R^3$ in Mij can be explained as follows:

$$p_e = \begin{bmatrix} x_e \\ y_e \\ \theta_e \end{bmatrix}_{(Mij)} = \begin{bmatrix} \cos \theta_c & \sin \theta_c & 0 \\ -\sin \theta_c & \cos \theta_c & 0 \\ 0 & 0 & 1 \end{bmatrix} \begin{bmatrix} x_r - x_c \\ y_r - y_c \\ \theta_r - \theta_c \end{bmatrix}_{(Oxy)} \\ = J_1(p_r - p_c)_{(Oxy)}, \quad (9)$$

where (x_e, y_e) is the phasor coordinate of MN in Mij and J_1 denotes the posture error transfer matrix, which transfers the posture error from Oxy to Mij . Obviously, the tracking error vector $(x_e, y_e, \theta_e) = 0$ if and only if $(x_c, y_c, \theta_c) = (x_r, y_r, \theta_r)$.

Differentiating the previous tracking error (9) and substituting \dot{p}_c by (8), differential equation of vehicle posture error can be derived as

$$\dot{p}_e = \begin{bmatrix} \dot{x}_e \\ \dot{y}_e \\ \dot{\theta}_e \end{bmatrix} = \begin{bmatrix} \omega_c y_e - v_c + v_r \cos \theta_e \\ -\omega_c x_e + v_r \sin \theta_e \\ \omega_r - \omega_c \end{bmatrix}, \quad (10)$$

where v_r, ω_r are reference linear velocity and angular velocity of vehicle, respectively.

3.2. Controller Design. The intelligent vehicle has the nature of nonholonomic constraint feature because the number of system inputs is less than the number of system outputs or system states. Lots of control methods are applied to control the nonholonomic systems, for example, linear feedback [21], fuzzy logic [22], variable structure [23], neural network [24], and so on [25]. There have no absolutely more predominant scheme than the others to resolve the nonholonomic problems presently though each of the control methods has advantages and disadvantages. Since the higher-dimensional and nonlinear characteristics of nonholonomic constraints, integral backstepping technology is often used to derive the controller of the intelligent vehicle.

In this paper, the complex nonlinear system is split into several subsystems whose number is less than system rank. Then the Lyapunov functions are constructed and the virtual controller of each subsystem is designed. Finally, the controller which is uniformly and ultimately bounded could be achieved by integrator recession and gradual correction. Therefore, the issue of trajectory tracking for lane changing on curved road based on system kinematics model could be transformed to find an appropriated control input $u_c = [v_c \ \omega_c]^T$ under any initial error; then to track reference posture $p_r = [x_r \ y_r \ \theta_r]^T$ and input $u_r = [v_r \ \omega_r]^T$, such that the tracking error space $p_e = [x_e \ y_e \ \theta_e]^T$ is abounded and satisfies that

$$\lim_{t \rightarrow \infty} [|x_e(t)| + |y_e(t)| + |\theta_e(t)|] = 0. \quad (11)$$

In the tracking error model (10), the lateral position error y_e cannot be directly controlled. To overcome this difficulty, this paper defines a new virtual variable \bar{x}_e by using integral backstepping [26], which is as follows:

$$\bar{x}_e = x_e - k_1 \frac{2n_1 \omega_c}{1 + \omega_c^2} y_e, \quad (12)$$

where k_1 and n_1 are positive constants and $k_1(2n_1 \omega_c / (1 + \omega_c^2)) y_e$ is virtual feedback parameter.

Differentiating (12) yields

$$\dot{\bar{x}}_e = \dot{x}_e - k_1 \frac{2n_1 - 2n_1 \omega_c^2}{\omega_c^4 + 2\omega_c^2 + 1} \dot{\omega}_c y_e - k_1 \frac{2n_1 \omega_c}{1 + \omega_c^2} \dot{y}_e. \quad (13)$$

In this case, when $x_e \rightarrow k_1(2n_1 \omega_c / (1 + \omega_c^2)) y_e$ and $\theta_e \rightarrow 0$, according to system (3), it obtains that

$$\dot{y}_e = -x_e \omega_c = -k_1 \frac{2n_1 \omega_c^2}{1 + \omega_c^2} y_e. \quad (14)$$

Suppose a Lyapunov function $V_y = (1/2)y_e^2$; note that differentiating this Lyapunov function is

$$\dot{V}_y = y_e \dot{y}_e = -k_1 \frac{2n_1 \omega_c^2}{1 + \omega_c^2} y_e^2. \quad (15)$$

Obviously, $\forall t \in (0, +\infty)$, $\dot{V}_y \leq 0$, and then system (14) will be asymptotically stabilized as $t \rightarrow 0$. According to the proposed preliminary, the trajectory controller can be given as

$$u_c = \begin{bmatrix} v_c \\ \omega_c \end{bmatrix} = \begin{bmatrix} v_r \cos \theta_e - k_1 \frac{2n_1 - 2n_1\omega_c^2}{\omega_c^4 + 2\omega_c^2 + 1} \dot{\omega}_c y_e + k_1 \frac{2n_1\omega_c^2}{1 + \omega_c^2} x_e - k_1 v_r \frac{2n_1\omega_c}{1 + \omega_c^2} \sin \theta_e + k_2 x_e - k_1 k_2 \frac{2n_1\omega_c}{1 + \omega_c^2} y_e \\ \omega_r + 2k_3 v_r y_e \cos \frac{\theta_e}{2} + k_4 \sin \frac{\theta_e}{2} \end{bmatrix}, \quad (16)$$

where k_1, k_2, k_3 , and k_4 are all positive constants whose value could determine the control directly.

3.3. Stability Analysis. According to the above analysis, a candidate Lyapunov function is defined as follows:

$$V = \frac{1}{2} \bar{x}_e^2 + \frac{1}{2} y_e^2 + \frac{2}{k_3} \left(1 - \cos \frac{\theta_e}{2} \right), \quad (17)$$

with $k_3 > 0$ and \bar{x}_e given by (12). As can be directly verified; V is a positive-definite and lower bounded function. Differentiating (17) yields

$$\begin{aligned} \dot{V} &= \bar{x}_e \dot{\bar{x}}_e + y_e \dot{y}_e + \frac{1}{k_3} \sin \frac{\theta_e}{2} \dot{\theta}_e \\ &= \bar{x}_e \left(\dot{x}_e - k_1 \frac{2n_1 - 2n_1\omega_c^2}{\omega_c^4 + 2\omega_c^2 + 1} \dot{\omega}_c y_e - k_1 \frac{2n_1\omega_c}{1 + \omega_c^2} \dot{y}_e \right) \\ &\quad + y_e (-\omega_c x_e + v_r \sin \theta_e) + \frac{1}{k_3} \sin \frac{\theta_e}{2} (\omega_r - \omega_c) \\ &= \bar{x}_e \left[(\omega_c y_e - v_c + v_r \cos \theta_e) - k_1 \frac{2n_1 - 2n_1\omega_c^2}{\omega_c^4 + 2\omega_c^2 + 1} \dot{\omega}_c y_e \right. \\ &\quad \left. - k_1 \frac{2n_1\omega_c}{1 + \omega_c^2} (-\omega_c x_e + v_r \sin \theta_e) \right] \\ &\quad + y_e \left[\left(-\omega_c \left(\bar{x}_e + k_1 \frac{2n_1\omega_c}{1 + \omega_c^2} y_e \right) + v_r \sin \theta_e \right) \right] \\ &\quad + \frac{1}{k_3} \sin \frac{\theta_e}{2} (\omega_r - \omega_c) \\ &= \bar{x}_e \left[v_r \cos \theta_e - v_c - k_1 \frac{2n_1 - 2n_1\omega_c^2}{\omega_c^4 + 2\omega_c^2 + 1} \dot{\omega}_c y_e \right. \\ &\quad \left. - k_1 \frac{2n_1\omega_c}{1 + \omega_c^2} (-\omega_c x_e + v_r \sin \theta_e) \right] \\ &\quad - k_1 \frac{2n_1\omega_c^2}{1 + \omega_c^2} y_e^2 \\ &\quad + \frac{1}{k_3} \sin \frac{\theta_e}{2} \left[(\omega_r - \omega_c) + 2k_3 v_r y_e \cos \frac{\theta_e}{2} \right]. \end{aligned} \quad (18)$$

Substituting (16) into (18) yields

$$\dot{V} = -k_2 \bar{x}_e^2 - k_1 \frac{2n_1\omega_c^2}{1 + \omega_c^2} y_e^2 - \frac{k_4}{k_3} \sin^2 \frac{\theta_e}{2}. \quad (19)$$

Note that k_1, k_2, k_3 , and k_4 are all positive constants and $2n_1\omega_c^2/(1 + \omega_c^2) > 0$, obviously, $\dot{V} \leq 0$ for $\forall t \in (0, +\infty)$ according to (19). V is a class of function which has the characteristic of being continuously differentiable, positive definite, and bounded, so \dot{V} is a negative semidefinite and uniformly continuous function.

Barbalat's lemma plays a key role in Lyapunov stability theory. Its basic theory is as follows. If a function $F(t, x)$ satisfies the following conditions: $F(t, x)$ is lower bounded and $\dot{F}(t, x)$ is negative semidefinite and uniformly continuous in time, then $\dot{F}(t, x) \rightarrow 0$ as $t \rightarrow \infty$. According to Barbalat's lemma, if $\dot{V} \rightarrow 0$ with $t \rightarrow \infty$, which is equivalent to that

$$\begin{aligned} \bar{x}_e^2 &\rightarrow 0, & y_e^2(t) &\rightarrow 0, \\ \frac{2n_1\omega_c}{1 + \omega_c^2} y_e(t) &\rightarrow 0, & \sin^2 \frac{\theta_e}{2} &\rightarrow 0. \end{aligned} \quad (20)$$

If $\sin^2(\theta_e/2) \rightarrow 0$, then

$$\lim_{t \rightarrow \infty} \theta_e \rightarrow 0 \quad (\theta_e \in [-\pi, \pi]), \quad (21)$$

while $\lim_{t \rightarrow \infty} \bar{x}_e = 0$, that is to say,

$$x_e \rightarrow k_1 \frac{2n_1\omega_c}{1 + \omega_c^2} y_e(t). \quad (22)$$

For the reason that v_r and ω_r are equal to zero with asynchronism, while ω_c is not identically zero and $k_1(2n_1\omega_c/(1 + \omega_c^2))y_e(t) \rightarrow 0$ based on the control law, so $y_e \rightarrow 0$.

Analyses above indicate that $x_e \rightarrow 0$. $\theta_e \in [-\pi, \pi]$ is equivalent to $\theta_e \in [0, +\infty)$ because θ_e is a periodic function. Obviously, according to Barbalat's lemma and Russell's invariant principle, it can be concluded that tracking errors $p_e = [x_e \ y_e \ \theta_e]^T$ is globally, uniformly, and ultimately bounded. Therefore, with the controller (16), we can get $\lim_{t \rightarrow \infty} [|x_e(t)| + |y_e(t)| + |\theta_e(t)|] = 0$. That is to say, the designed trajectory tracking controller for the above lane changing maneuver has characteristics of global stability.

4. Simulation and Discussion

This paper performs a computer simulation on the intelligent vehicle by using the designed controller to tracking the predefined lane changing trajectory on curved roads. A brief diagram for this controller can be described by Figure 4.

According to the standard of roadway designing manual when design the highway alignment, it is necessary to establish the proper relation between design speed and curvature. The minimum radii of curves are important control values

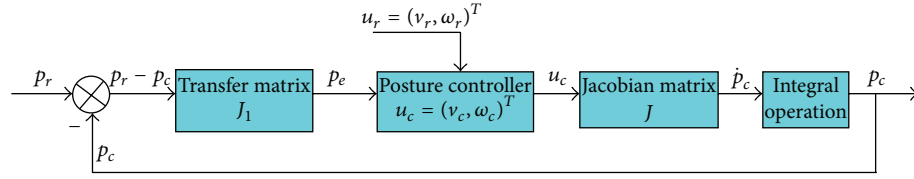


FIGURE 4: Schematic diagram of vehicle's control system structure.

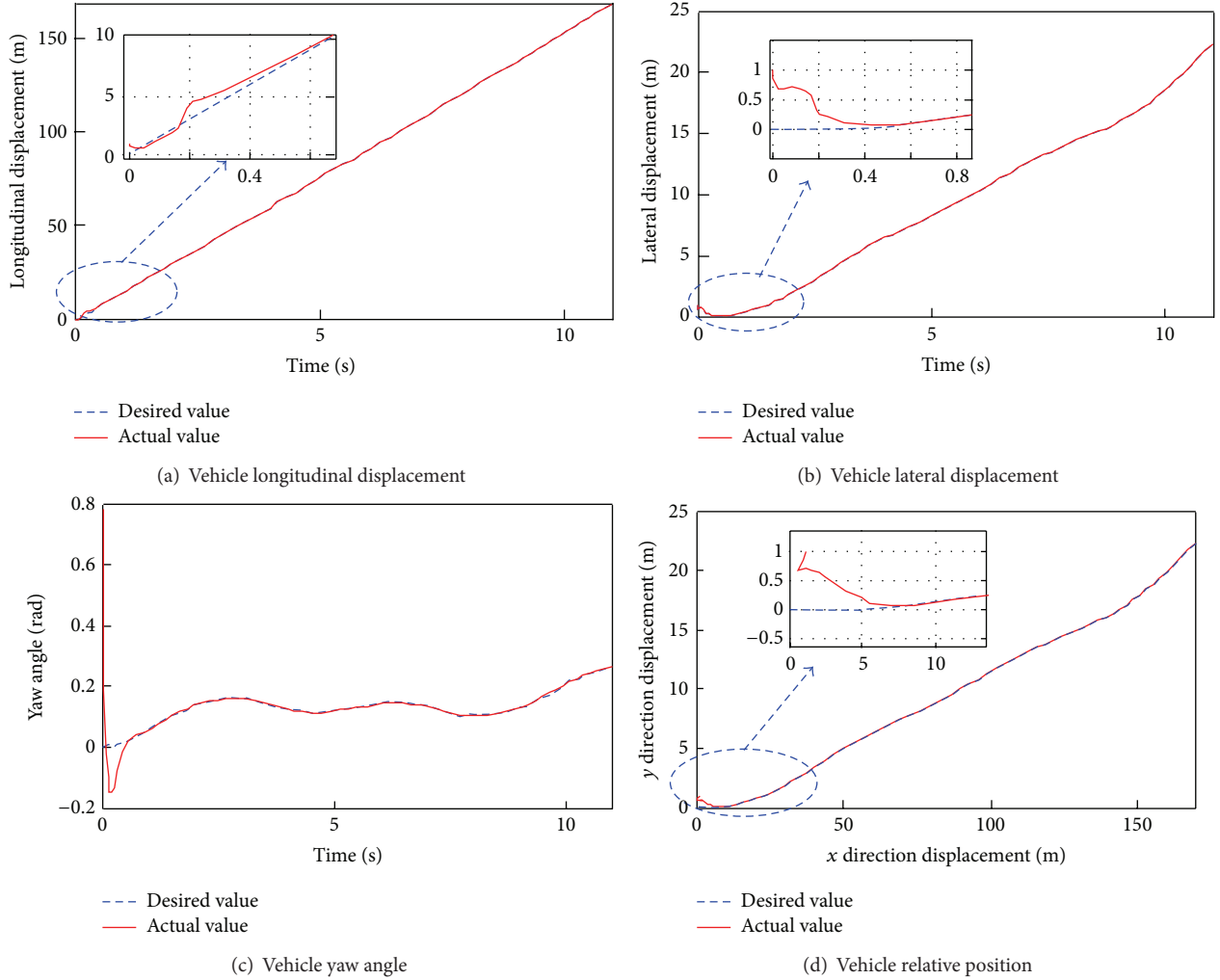


FIGURE 5: Trajectory tracking simulation results for lane changing.

in designing for safe operation. For example, when the design speed of road is higher than 100 km/h, then the usual minimum radius of curve must be longer than 650 m. The common width of the lane on highway is 3.75 m. The target of this paper is to guarantee the safety of intelligent vehicle on highway curved roads with high speed. Therefore, the parameters for the simulation scenarios are set considering the above specifications.

The curvature radius of the outside lane R is set to be 650 m, the space between the outside and inside lane d_w is 3.75 m, and the maximum of the desired lateral jerk J_{\max} is 0.1 g/s. We can get that $t_1 = 1$ s, $t_2 = 1.5$ s from (2), so the time needed for lane changing is $t_5 = 5$ s. Here,

the gravity acceleration $g = 10 \text{ m/s}^2$. In the simulation, the initial values of the desired longitudinal displacement and longitudinal velocity are 0 and 15 m/s, respectively, the longitudinal acceleration $\dot{v}_d(t)$ is described as (3), and the initial tracking error $[x_e \ y_e \ \theta_e]^T = [-1 \ -1 \ -\pi/4]^T$.

As a report from National Highway Traffic Safety Administration indicates, most lane changes are with a mean duration of over 11 s. Besides, to reflect the influence of radius difference between the outside and inside lane on lane changing trajectory, the process of the lane changing maneuver was divided into three steps. Step 1 conducts the action from the outside to the inside lane duration from 1–5 s. During step 2, the vehicle runs along the inside lane so as

TABLE 1: Parameters of the controller.

| Symbol | k_1 | k_2 | k_3 | k_4 | n_1 |
|--------|-------|-------|-------|-------|-------|
| Value | 1.5 | 2 | 2 | 2.5 | 1 |

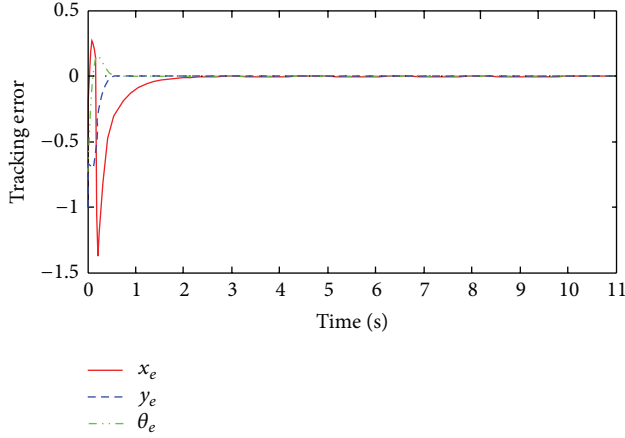


FIGURE 6: Trajectory tracking error for lane changing.

to avoid continuous lane changing maneuver. Step 3 conducts the action from the inside to the outside lane duration from 6–11 s. Therefore, the simulation time of the lane changing maneuver was set to be 11 s. The control parameters of the simulation are shown in Table 1.

The corresponding simulation results are given in Figures 5 and 6. Figure 5 is shown as the trajectory tracking simulation curves of lane changing, where the dotted lines are the desired states of lane changing and the solid lines denote the actual states.

Figures 5(a), 5(b), and 5(c) denote changes of the longitudinal displacement, the lateral displacement, and the yaw angle with process time t for lane changing on curved road, respectively. As can be seen from the figures above, these 3 actual states can all realize the tracking of corresponding desired state at about 0.6 s. Figure 5(d) is the x - y trajectory tracking curve, which describes the lane changing trajectory on curved road in Oxy ; from the local enlarging graphs of this figure, we can get that the desired lane changing trajectory could be tracked effectively after longitudinal driving about 10 m.

The change of tracking error x_e , y_e , and θ_e with process time t is shown in Figure 6.

As shown in Figure 6, these 3 tracking errors described intelligent vehicle system all converge to zero asymptotically under the function of trajectory tracking controller. Simulation results demonstrate that the controller has characteristics of quick convergence and global stability, and it can realize ideal tracking of lane changing trajectory on curved road. Figure 7 displays the steering angle of the vehicle during the lane change maneuver.

Figure 8 shows the system control inputs, where (a) denotes the linear velocity input and (b) indicates the angular velocity input. The control input $u_c = [v_c \ \omega_c]^T$ tends to be stable at about 0.6 s in lane changing maneuver, and the intelligent vehicle system is globally stable. Additionally, from

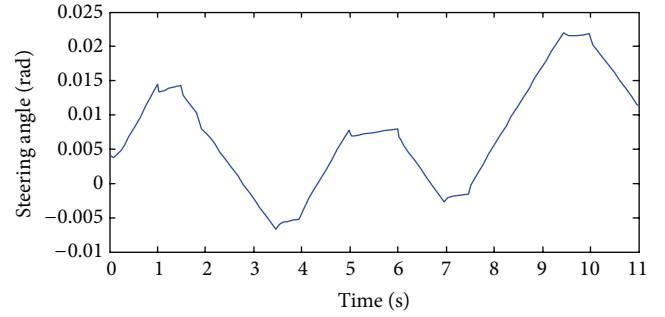


FIGURE 7: The steering angle of the intelligent vehicle.

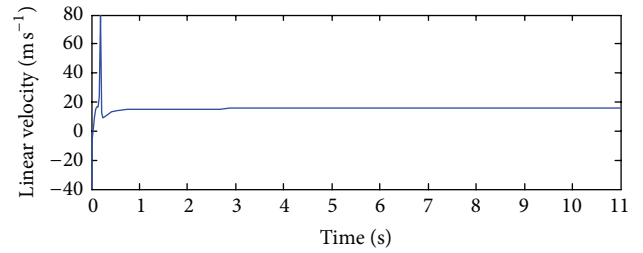
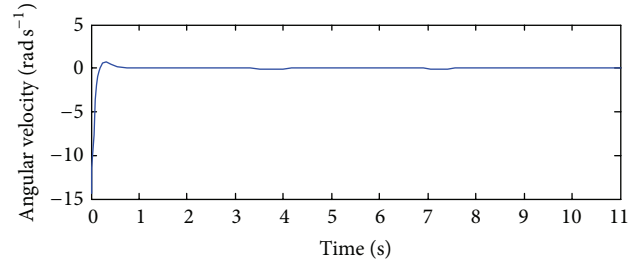
(a) Controller input of linear velocity u_c (b) Controller input of angular velocity ω_c

FIGURE 8: Inputs curves of the tracking controller.

(a) and (b), it can be seen that $|u_c|_{\max} = 16$ m/s and $|\omega_c|_{\max} = 0.08$ rad/s, which makes the control smoothing in vehicle's lane changing maneuver. Meanwhile, the linear velocity when driving along the inside lane is 15.5 m/s and the angular velocity is 0.02 rad/s.

5. Conclusions

In this paper, a lane changing trajectory is planned and tracked for lane changing of an intelligent vehicle on curved road. From the development in the previous sections and the simulation results above, we have the following conclusions.

(1) Taking into account the difference of curvature radius between the outside and inside lane, this paper utilizes the trajectory planning method based on trapezoidal acceleration profile to meet the restriction of the various curvatures and change rate for lane changing on curved road. Then it considers the coupled function of the vehicle's longitudinal and lateral motion on lane changing trajectory, namely, the curvature radius of which is a vector in lane changing maneuver. In order to track smoothly to a given trajectory,

the tracking error function is generated by a vector between the predictive reference vector and the vehicle real posture, which is derived from the velocity equation.

(2) Aiming to figure out the nonholonomic constraints of the tracking model and the strong coupling between vehicle's longitudinal and lateral motion, the trajectory tracking control algorithm is designed using integral backstepping with intermediate virtual controllers, which is devoted to the research of trajectory tracking for lane changing on curved road. Simulation results demonstrate that this controller can guarantee the convergences of both the relative position tracking errors and the position tracking synchronization.

Simulations have been carried out to demonstrate the effectiveness of the proposed control methods, but relevant tracking experiments on the intelligent vehicle prototype should be performed on the intelligent vehicle. Next step, we will concentrate on that to test and verify simulation results.

Conflict of Interests

The authors declare that there is no conflict of interests regarding the publication of this paper.

Acknowledgments

This research was financed by the National Natural Science Foundation of China (51305065 and 61175101), the Urumqi City Science and Technology Project (G121310001) and the Fundamental Research Funds for the Central Universities (DUT13JS02 and DUT13JS14).

References

- [1] R. Gregor, M. Lützel, M. Pellkofer, K.-H. Siedersberger, and E. D. Dickmanns, "EMS-vision: a perceptual system for intelligent vehicles," *IEEE Transactions on Intelligent Transportation Systems*, vol. 3, no. 1, pp. 48–59, 2002.
- [2] K. Choi, S. Park, S. Kim et al., "Methods to detect road features for video-based in-vehicle navigation systems," *Journal of Intelligent Transportation Systems*, vol. 14, no. 1, pp. 13–26, 2010.
- [3] R. Sengupta, S. Rezaei, S. E. Shladover, D. Cody, S. Dickey, and H. Krishnan, "Cooperative collision warning systems: concept definition and experimental implementation," *Journal of Intelligent Transportation Systems*, vol. 11, no. 3, pp. 143–155, 2007.
- [4] L. Cai, A. B. Rad, and W. Chan, "An intelligent longitudinal controller for application in semiautonomous vehicles," *IEEE Transactions on Industrial Electronics*, vol. 57, no. 4, pp. 1487–1497, 2010.
- [5] B. Yu, Z. Z. Yang, and L. I. S., "Real-time partway deadheading strategy based on transit service reliability assessment," *Transportation Research A*, vol. 46, no. 8, pp. 1265–1279, 2012.
- [6] J. E. Naranjo, C. González, R. García, and T. de Pedro, "Lane-change fuzzy control in autonomous vehicles for the overtaking maneuver," *IEEE Transactions on Intelligent Transportation Systems*, vol. 9, no. 3, pp. 438–450, 2008.
- [7] D. B. Ren, J. Y. Zhang, J. M. Zhang, and S. M. Cui, "Trajectory planning and yaw rate tracking control for lane changing of intelligent vehicle on curved road," *Science China Technological Sciences*, vol. 54, no. 3, pp. 630–642, 2011.
- [8] D. Soudbakhsh, A. Eskandarian, and D. Chichka, "Vehicle steering maneuvers with direct trajectory optimization," in *Proceedings of the IEEE Intelligent Vehicles Symposium (IV '10)*, pp. 449–453, San Diego, Calif, USA, June 2010.
- [9] C. S. Yang, Z. Yang, X. N. Huang, S. B. Li, and Q. Zhang, "Modeling and robust trajectory tracking control for a novel six-rotor unmanned aerial vehicle," *Mathematical Problems in Engineering*, vol. 2013, Article ID 673525, 13 pages, 2013.
- [10] C. Hatipoglu, Ü. Özgüner, and K. A. Redmill, "Automated lane change controller design," *IEEE Transactions on Intelligent Transportation Systems*, vol. 4, no. 1, pp. 13–22, 2003.
- [11] S. Ammoun, F. Nashashibi, and C. Laureau, "An analysis of the lane changing manoeuvre on roads: the contribution of inter-vehicle cooperation via communication," in *Proceedings of the IEEE Intelligent Vehicles Symposium (IV '07)*, pp. 1095–1100, Istanbul, Turkey, June 2007.
- [12] T. Lee, B. Kim, K. Yi, and C. Jeong, "Development of lane change driver model for closed-loop simulation of the active safety system," in *Proceedings of the 14th IEEE International Intelligent Transportation Systems Conference (ITSC '11)*, pp. 56–61, Washington, DC, USA, October 2011.
- [13] R. Toledo-Moreo and M. A. Zamora-Izquierdo, "IMM-based lane-change prediction in highways with low-cost GPS/INS," *IEEE Transactions on Intelligent Transportation Systems*, vol. 10, no. 1, pp. 180–185, 2009.
- [14] M. L. Ho, P. T. Chan, and A. B. Rad, "Lane change algorithm for autonomous vehicles via virtual curvature method," *Journal of Advanced Transportation*, vol. 43, no. 1, pp. 47–70, 2009.
- [15] F. You, R. Wang, R. Zhang, and W. Xiong, "Lane changing and overtaking control method for intelligent vehicle based on backstepping algorithm," *Transactions of the Chinese Society of Agricultural Machinery*, vol. 39, no. 6, pp. 42–45, 2008.
- [16] B. Z. Yao, P. Hu, M. H. Zhang, and S. Wang, "Artificial bee colony algorithm with scanning strategy for periodic vehicle routing problem," *SIMULATION*, vol. 89, no. 6, pp. 762–770, 2013.
- [17] J. Ackermann, J. Guldner, W. Sienel, R. Steinhauser, and V. I. Utkin, "Linear and nonlinear controller design for robust automatic steering," *IEEE Transactions on Control Systems Technology*, vol. 3, no. 1, pp. 132–143, 1995.
- [18] M. A. Sotelo, E. Naranjo, R. García, T. D. Pedro, and C. González, "Comparative study of chained systems theory and fuzzy logic as a solution for the nonlinear lateral control of a road vehicle," *Nonlinear Dynamics*, vol. 49, no. 4, pp. 463–474, 2007.
- [19] R. Rajamani, H. Tan, B. K. Law, and W. Zhang, "Demonstration of integrated longitudinal and lateral control for the operation of automated vehicles in platoons," *IEEE Transactions on Control Systems Technology*, vol. 8, no. 4, pp. 695–708, 2000.
- [20] J. Lee and W. Yoo, "An improved model-based predictive control of vehicle trajectory by using nonlinear function," *Journal of Mechanical Science and Technology*, vol. 23, no. 4, pp. 918–922, 2009.
- [21] Z. Li, S. S. Ge, M. Adams, and W. S. Wijesoma, "Robust adaptive control of uncertain force/motion constrained nonholonomic mobile manipulators," *Automatica*, vol. 44, no. 3, pp. 776–784, 2008.
- [22] D. Chwa, "Sliding-mode tracking control of nonholonomic wheeled mobile robots in polar coordinates," *IEEE Transactions on Control Systems Technology*, vol. 12, no. 4, pp. 637–644, 2004.

- [23] T. Das and I. N. Kar, "Design and implementation of an adaptive fuzzy logic-based controller for wheeled mobile robots," *IEEE Transactions on Control Systems Technology*, vol. 14, no. 3, pp. 501–510, 2006.
- [24] C. X. Ding, W. H. Wang, X. Wang, and M. Baumann, "A neural network model for driver's lane-changing trajectory prediction in urban traffic flow," *Mathematical Problems in Engineering*, vol. 2013, Article ID 967358, 8 pages, 2013.
- [25] B. Yao, C. Yang, J. Yao, and J. Sun, "Tunnel surrounding rock displacement prediction using support vector machine," *International Journal of Computational Intelligence Systems*, vol. 3, no. 6, pp. 843–852, 2010.
- [26] A. Rantzer, "A dual to Lyapunov's stability theorem," *Systems and Control Letters*, vol. 42, no. 3, pp. 161–168, 2001.

